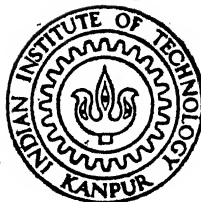


FINITE ELEMENT ANALYSIS OF PLANER BED - 'CARRIAGE INTERFACE AS A CONTACT PROBLEM'

by
NAVIN VERMA



DEPARTMENT OF MECHANICAL ENGINEERING
INDIAN INSTITUTE OF TECHNOLOGY, KANPUR

1990

MA
1990
M
VER
FIN

FINITE ELEMENT ANALYSIS OF PLANER BED - 'CARRIAGE INTERFACE AS A CONTACT PROBLEM'

A Thesis Submitted
in Partial Fulfilment of the Requirements
for the Degree of
MASTER OF TECHNOLOGY

by
NAVIN VERMA

to the
DEPARTMENT OF MECHANICAL ENGINEERING
INDIAN INSTITUTE OF TECHNOLOGY, KANPUR
1990

ME-1190-M-VER-FIN.

13 SEP 1990

CENTRAL LIBRARY
J. I. T. KANPUR


Acc. No. A108874

Th
621.89
V 59 6

21/12/83
B

CERTIFICATE

This is to certify that the thesis entitled, 'Finite Element Analysis of Planer Bed - Carriage Interface as a Contact Problem', by Navin Verma is a bonafide record of work done by him under my guidance and supervision and has not been submitted elsewhere for the award of a degree.


(P. M. Dixit)
Assistant Professor
Dept. of Mechanical Engg.
Indian Institute of Technology,
Kanpur 208 016

ACKNOWLEDGEMENTS

I thank Dr. P.M. Dixit with sincerity and gratitude for his valuable guidance at various stages of my thesis. His encouragement and perseverance helped me attain my goal. I also thank my friends for the company and support they provided throughout the endeavour.

Navin Verma

CONTENTS

	<u>Page</u>
LIST OF FIGURES	ii
LIST OF TABLES	iii
NOMENCLATURE	iv
ABSTRACT	vii
CHAPTER I INTRODUCTION	1
1.1 Machine tool joints	1
1.2 Literature survey	1
1.2.1 Deformation determination methods	2
1.2.2 FEM for solving contact problems	2
1.3 Objective and scope of work	3
1.4 Plan of thesis	5
CHAPTER II FINITE ELEMENT ALGORITHM	6
2.1 FEM formulation for Plane Strain	6
2.2 Formulation for contact problems	12
2.3 Contact conditions	12
2.4 Application of contact conditions	15
2.5 Substructuring	17
2.6 Program Algorithm	19
2.7 Stress evaluation	20
CHAPTER III RESULTS AND DISCUSSIONS	22
3.1 Flat plate over a flat plate	22
3.2 Planer bed - carriage contact problem	26
CHAPTER IV CONCLUSIONS AND SUGGESTIONS FOR FUTURE WORK	42
4.1 Conclusions	42
4.2 Suggestlons for future work	43
REFERENCES	44

LIST OF FIGURES

<u>Figure</u>	<u>Title</u>	<u>Page</u>
2.1	Body in plane strain	7
2.2	Discretisation of the domain	7
2.3	Bodies in contact	13
2.4	Rearranged Matrix	13
3.1	(a) Flat plate over flat plate configuration	23
	(b) Finite element mesh and the deformation	24
	(c) Normal stress variation for different μ	25
3.2	(a) V-Joint of a planer	27
	(b) Finite element mesh	28
3.3	Deformation pattern	30
3.4	Variation of normal displacements along the contact length for different values of μ	
	(a) Force at location 1	31
	(b) Force at location 2	31
	(c) Force at location 3	31
	(d) Force at location 4	31
3.5	Variation of tangential displacements along the contact length of bed for different values of μ	
	(a) Force at location 1	32
	(b) Force at location 2	32
	(c) Force at location 3	32
	(d) Force at location 4	32
3.6	Variation of tangential displacements along the contact length of carriage for different values of μ	
	(a) Force at location 1	33
	(b) Force at location 2	33
	(c) Force at location 3	33
	(d) Force at location 4	33
3.7	Variation of normal and shear stress along the contact length for different value s of μ	
	(a) Force at location 1	34
	(b) Force at location 2	35
	(c) Force at location 3	36
	(d) Force at location 4	37

LIST OF TABLES

<u>Table</u>	<u>Title</u>	<u>Page</u>
A	Case (1) data	38
B	Case (2) data	39
C	Case (3) data	39
D	Case (4) data	40

NOMENCLATURE

A	Body A
A_e	Element Area
B	Body B
B_x, B_y	Components of body force vector
C	Surface finish constant
dA	Elemental area
dl	Element length
E	Young's Modulus
F_x, F_y	Components of surface force vector with respect to x-y axis
t_n, t_s	Components of surface force vector with respect to n-s axis
m	Material constant
N_e	Number of elements
N_i	Shape functions
N_b	Number of elements having boundary force specified
n	Normal to boundary
n_x, n_y	Components of normal with respect to xy axes
P	Load per unit axial length
s	Tangent to boundary
U	Strain Energy
u	Displacement in x-direction
v	Displacement in y-direction
W_p	Work done by external forces

$x-y$	Cartesian coordinates
$Z-Z$	Axis of symmetry
α	Angle made by s -direction with X -axis
Γ	System boundary
Γ_q	Boundary with specified forces
ϵ_{xy}	Shear strain with respect to xy component
ϵ	Clearance
ϵ_x, ϵ_y	Normal strains in x & y directions
Ω	Domain of the problem
Ω_e	Elemental domain
μ	Coefficient of friction
μ_m	Microns
ν	Poisson's ratio
π_p	Potential energy
σ_x, σ_y	Normal stress in x - y directions
τ_{xy}	Shear stress with respect to X - Y directions
$[\]$	Matrix
$\{ \}$	Vector
$[B]$	Shape function derivative matrix
$[D]$	Material constants matrix
$\{B_f\}$	Body force vector
$\{F\}$	Global force vector
$[F_A], [F_B]$	Force vector for Body A & B
$[f]^e$	Elemental body force vector
$\{f_s\}$	Surface force (stress) vector
$[K]$	Global stiffness matrix
$[k]^e$	Elemental stiffness matrix

$[K_A]$	Global stiffness matrix of body A
$[K_B]$	Global stiffness matrix of body B
$[N]$	Matrix containing shape functions
$\{U\}$	Global nodal displacement vector
$\{U_A\}$	Global nodal displacement vector of body A
$\{U_B\}$	Global nodal displacement vector of body B
$\{u\}$	Displacement vector
$\{u\}_{nodal}^e$	Nodal displacements vector of an element
$\{u\}_{nodal}^b$	Nodal displacement vector for a boundary element
$\{\epsilon\}$	Strain vector
$\{\sigma\}$	Stress vector

ABSTRACT

The unknown boundary conditions at the machine tool bed-carriage interface make it difficult to analyse the joint. At the contact nodes both the displacements as well as forces are unknown. Depending on the contact forces and the coefficient of friction, the nodes will either slip or adhere to each other during deformation. The deformation may also render some nodes out of contact.

In this work, a solution procedure to analyse the contact problems with varying coefficient of friction is developed using the finite element technique. This is further used to analyse the V-slide joint of a planer bed for studying the deflections and stresses for different values of coefficient of friction, and different points of application of the applied force.

CHAPTER I

INTRODUCTION

1.1 MACHINE TOOL JOINTS:

Machine tool joints may be classified as fixed joint such as bolted connections, shrink fit assemblies, etc. or sliding joints such as various types of guideways. Various forces including the frictional forces are transmitted across the interface which cause elastic displacements. The interface displacements influence the overall displacements of the machine tool members. Tilting of the slides due to deformation affects the operating properties of the slideways.

It is essential to know the deflections as they have a profound influence on the machine tool operational accuracy. From strength point of view, it is necessary to know whether the stresses are below the safe levels. In particular shear stress plays an important role in wear of contact surfaces.

1.2 LITERATURE SURVEY

1.2.1 Methods for Determining Contact Deformations:

For determining the pressure distribution at the contact surface and the deformations due to external load N. Back, M. Burdekin and A. Cowley [1] proposed an iterative approach. In this approach, the compliance of the contact surface is assumed nonlinear as given by the relation:

$$\lambda = C (100 p)^m \quad (1.1)$$

where

λ = approach of surface in μm

C, m = constants depending on material and surface finish characteristics

p = pressure

The contact between the components is simulated using springs or plates with properties which are taken as functions of surface roughness, pair of materials and pressure distribution. This method however has limited application as it relies on the empirical relation (1.1). Further, it does not take into account the effect of friction.

Another approach of calculating stresses and deformation in machine tool joints is to analyse the joint as a contact problem. Various classical solutions for this special class of solid mechanics problems are available. In three dimensions, the problem of contact of two elastic bodies was first formulated and solved by Hertz [2] under several restrictive assumptions. The Hertz problem was reduced to an integral equation and solved by Mushkhelishvili [3] and Gladwell [4]. However, the complex geometries of machine tool joints are extremely difficult to model in the conventional way. Here finite element methods plays an important role in analysing such complicated geometries and boundary conditions.

1.2.2 Finite Element Methods for Contact Problems:

The earliest application of finite element method to contact problem appears to be in the paper of Chan and Tuba [5]. S. Ohte [6] proposed a method in which the contact interface is classified

into adhering and sliding states according to reaction force acting on the contact surface and the friction coefficient. Francavilla and Zienkiewicz [7] solved the frictionless case of contact problems as a quasilinear problem. Hung and Sauxe [8] used finite element method and mathematical programming techniques to solve frictionless contact problems. Here appropriate linearization of contact conditions is adopted and solved as a non-iterative optimisation problem. Sachdeva, Ramakrishnan and Natrajan extended the method of Francavilla and Zienkiewicz to take into account the force boundary conditions [9] and frictional effects under proportionate loading [10], Torstenfelt [11] proposed a general purpose finite element computer program to solve contact problems with friction. P.V. Kishore [12] proposed the minimization of dissipation energy approach for solving contact problems. Here the extent of slip is determined by the minimisation of the dissipation energy function.

The approach suggested by Sachdeva and Ramakrishnan [10] has been modified in the present work. They have used flexibility matrix, whereas in the present approach the contact conditions are applied to the stiffness matrix. Besides this, the matrix substructuring technique proposed by P.V. Kishore [12], is utilized for optimum storage and computational efficiency.

1.3 OBJECTIVE AND SCOPE OF PRESENT WORK:

The present work describes an iterative numerical procedure to solve two dimensional elastic contact problems with friction using the conventional stiffness matrix. This stiffness matrix is condensed using a substructuring algorithm to eliminate all the nodes except those which are likely to be in contact and those

where there are external forces acting. To begin with a set of nodes is assumed to be in contact. Newton's third law is applied to nodal forces and the compatibility conditions are applied to both the normal and tangential nodal displacements. In the subsequent iteration, the contact conditions are dropped for the nodes going out of contact and for the slipping nodes, the displacement compatibility is applied only in the normal direction while the slip condition is applied in the tangential direction. Stresses at the contact surface are obtained by averaging the stresses over the bodies in contact. The iterative scheme converges very fast.

The method presented here is first applied to a simple problem with known solution to test its applicability, followed by the planer tool bed-carriage V-joint problem. The two bodies in contact are the portions of carriage and the bed. Although the cutting force has both the components, only the vertical component is considered in analysis. It is assumed that the horizontal force will not affect much the pattern of deformation/stresses in the contact region. The above assumption helps us in idealising the configuration as a plane strain problem whereby only a thin slice of the body needs to be analysed. Only half the carriage-bed structure is considered by assuming symmetric loading conditions and imposing suitable boundary conditions at the line of symmetry. The three cases of coefficient of friction account for the dry metal to metal contact and boundary lubrication conditions.

The limitations of the method may be summarized as follows:

- (a) The contact conditions for the two bodies are applied only at the nodes, whereas ideally they have to be applied over the entire contact length.
- (b) The cutting forces have been assumed to act at a point whereas in actual conditions there is a finite width of cut.
- (c) Body forces have been neglected in the present analysis as their magnitude is small as compared to the cutting force.
- (d) Incremental loading has not been considered. But in starting operations, the magnitude of cutting force actually increases from zero to a peak value.

Since the problem has been idealised as a 2-D problem, the results are valid only in the middle portion of the carriage where plane strain conditions are more or less valid. However, the actual problem is 3-Dimensional. The effect of the horizontal forces can also be studied only in a 3-Dimensional analysis.

1.4 PLAN OF THE THESIS:

Chapter II deals with the finite element formulation of a contact problem. It describes the details of the substructuring and the application of the contact conditions. The results and discussion are given in Chapter III. The work concludes in Chapter IV with the suggestions for future work.

CHAPTER II

FINITE ELEMENT ALGORITHM

This chapter presents the finite element formulation of elastic bodies in contact for plane strain conditions. In particular, it describes the matrix substructuring technique where a condensed stiffness matrix is obtained from the stiffness matrices of bodies in contact in skyline form. Besides, the contact conditions algorithm is also discussed.

2.1 FEM FORMULATION FOR PLANE STRAIN

When a cylindrical body is subjected to support conditions and external forces which have no components along the axis of the cylinder and the remaining components do not change along the axis, the body is said to be in a state of plane strain. If the Z-coordinate is taken along the axis of the cylinder, then the displacement, stress and strain components (with the exception of σ_z) associated with the Z-direction are zero and the remaining components are independent of Z. Then it is sufficient to analyse only a thin slice of the body.

Figure 2.1 shows a slice of thickness h of a cylindrical body in a state of plane strain. Let Ω be the region occupied by the cross-section of the slice and Γ be its boundary. The part of the boundary on which the external forces act is denoted by Γ_q .

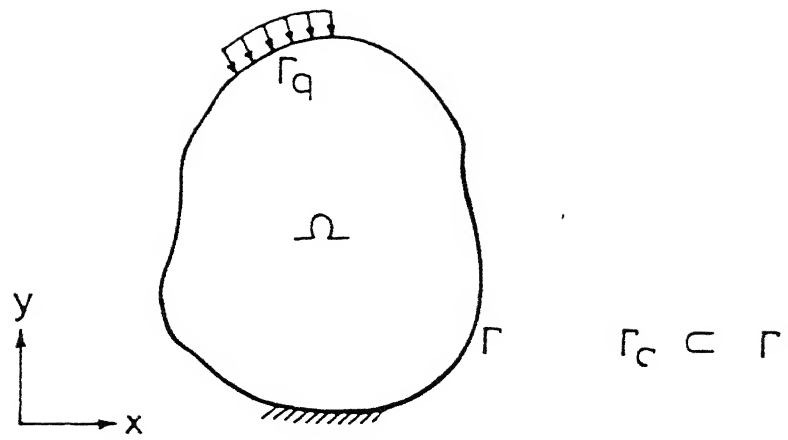


Fig.2.1 Body in plane strain.

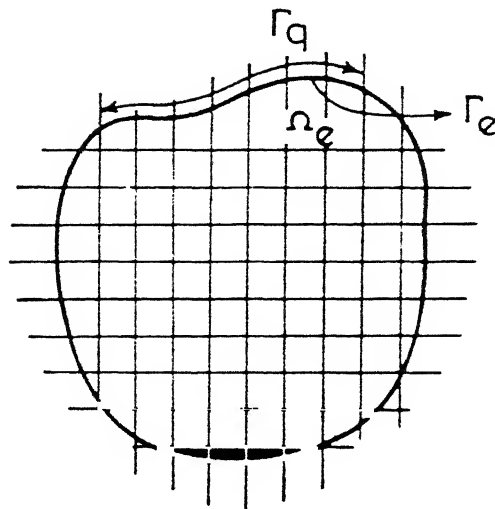


Fig.2.2 Discretisation of the domain.

The relation between the non-zero strain and displacement components is given by

$$\epsilon_x = \frac{\partial u}{\partial x}; \epsilon_y = \frac{\partial v}{\partial y}; \epsilon_{xy} = \frac{\partial u}{\partial y} + \frac{\partial v}{\partial x} \quad (2.1)$$

If we write the strain and displacement components as

$$\{\epsilon\} = \begin{Bmatrix} \epsilon_x \\ \epsilon_y \\ \epsilon_{xy} \end{Bmatrix}, \quad \{u\} = \begin{Bmatrix} u \\ v \end{Bmatrix} \quad (2.2)$$

then this relation becomes

$$\{\epsilon\} = \begin{bmatrix} \frac{\partial}{\partial x} & 0 \\ 0 & \frac{\partial}{\partial y} \\ \frac{\partial}{\partial y} & \frac{\partial}{\partial x} \end{bmatrix} \begin{Bmatrix} u \\ v \end{Bmatrix} \quad (2.3)$$

If the stress components σ_x , σ_y , τ_{xy} are also arranged in a vector form

$$\{\sigma\} = \begin{Bmatrix} \sigma_x \\ \sigma_y \\ \tau_{xy} \end{Bmatrix}, \quad (2.4)$$

Then the stress-strain relation for a linearly elastic material under plane strain conditions, becomes

$$\{\sigma\} = [D] \{\epsilon\} \quad (2.5)$$

where $[D]$ is given by

$$[D] = \frac{E(1-\nu)}{(1+\nu)(1-2\nu)} \begin{bmatrix} 1 & \nu/(1-\nu) & 0 \\ \nu/(1-\nu) & 1 & 0 \\ 0 & 0 & (1-2\nu)/2(1-\nu) \end{bmatrix} \quad (2.6)$$

where E is the Young's Modulus and

ν is the Poisson's ratio of the material.

The strain energy is given by the expression

$$\begin{aligned} U &= \int_{\Omega} \frac{1}{2} \{\epsilon\}^T \{D\} \{\epsilon\} h \, dA \\ &= \int_{\Omega} \frac{1}{2} \{\epsilon\}^T \{D\} \{\epsilon\} h \, dA \end{aligned} \quad (2.7)$$

$$\text{Let } \{f_s\} = \begin{Bmatrix} f_x \\ f_y \end{Bmatrix}, \quad \{B_f\} = \begin{Bmatrix} B_x \\ B_y \end{Bmatrix} \quad (2.8)$$

represent the applied traction on Γ_q and the body force (per unit volume) respectively, then the work done by the external forces is given by

$$W_p = \int_{\Omega} \frac{1}{2} \{B\}^T \{u\} h \, dA + \int_{\Gamma_q} \{f_s\}^T \{u\} h \, dA \quad (2.9)$$

The expression for potential energy of the system is given as

$$\pi_p = U - W_p$$

Hence

$$\begin{aligned} \pi_p &= \frac{1}{2} \int_{\Omega} \{\epsilon\}^T \{D\} \{\epsilon\} h \, dA - \int_{\Omega} \frac{1}{2} \{B_f\}^T \{u\} h \, dA \\ &\quad - \int_{\Gamma_q} \{f_s\}^T \{u\} h \, dA \end{aligned} \quad (2.10)$$

Let the domain be divided into N_e number of elements (Figure 2.2). Over a typical element Q_e , let

$$\{u\} = \begin{bmatrix} N_1 & 0 & \dots & N_n & 0 \\ 0 & N_1 & \dots & 0 & N_n \end{bmatrix} \begin{Bmatrix} u_1^e \\ v_1^e \\ \vdots \\ u_n^e \\ v_n^e \end{Bmatrix} = [N] \{u\}_{nodal} \quad (2.11)$$

be the approximation for the displacement vector. Here $u_1^e, v_1^e \dots u_n^e, v_n^e$ are the values of the displacements at the n nodes of the element while $N_1 \dots N_n$ are polynomial functions of the coordinates x and y , called the shape functions. From equation (2.3) we get

$$\{\epsilon\} = [B] \{u\}_{nodal}^e \quad (2.12)$$

where the matrix $[B]$ contains the derivatives of the shape functions. Substituting equations (2.11) and (2.12) into (2.10), the expression for potential energy can be written as

$$\begin{aligned} \pi_p = & \sum_{e=1}^{N_e} \frac{1}{2} \int_{\Omega_e} \{u\}_{nodal}^e [B]^T [D] [B] \{u\}_{nodal}^e h dA \\ & - \sum_{e=1}^{N_e} h \int_{\Omega_e} \{u\}_{nodal}^e [N]^T \{B_f\} dA \\ & - \sum_{b=1}^{N_b} h \int_{\Gamma_b} \{u\}_{nodal}^b [N']^T \{B_s\} dl \end{aligned} \quad (2.13)$$

Note that when the domain is divided into area elements, the boundary Γ_q automatically gets divided into line elements. N_b is the number of such line elements, Γ_b is the domain of a typical line element b and

$$\{u\} = \begin{bmatrix} N_1' & 0 & N_2' & \dots & N_n' & 0 \\ 0 & N_1 & 0 & N_2 & 0 & N_n \end{bmatrix} \begin{Bmatrix} u_1 & b \\ v_1 & b \\ \vdots & \\ u_n & b \\ v_n & b \end{Bmatrix} = [N]' \{u\}_{\text{nodal}}^b \quad (2.14)$$

is the approximation for the displacement vector over it. Setting the first variation of π_p to zero, we get

$$[K] \{U\} = \{F\}$$

where

$$[K] = \sum_{e=1}^{N_e} [k]^e \quad (\text{Stiffness Matrix})$$

$$[k]^e = \int_{\Omega_e} [B]^T [D] [B] h \, dA_e$$

$$\{F\} = \sum_{e=1}^{N_e} \{f\}^e + \sum_{b=1}^{N_b} \{f\}^b \quad (\text{Force Vector})$$

$$\{k\}^e = \int_{\Omega_e} [N]^T \{B_f\} h \, dA_e$$

$$\{f\}^b = \int_{\Gamma_b} [N]'^T \{f_s\} h \, dA_e$$

$$\{f\}^e = \int_{\Gamma_e} [N]^T \{B_f\} h \, dA_e \quad (2.15)$$

and $\{U\}$ is the vector of nodal displacements for the entire domain. In eq. (2.14) it is understood that the element matrix $[k]^e$ and element vectors $\{f\}^e$ and $\{f\}^b$ are first expanded to the full size before adding.

2.2 FORMULATION FOR CONTACT PROBLEMS:

Two bodies A and B which are in contact with each other are shown in Fig. 2.3. The finite element equations for these bodies are

$$\begin{aligned} [K_A] \{U_A\} &= \{F_A\} \\ [K_B] \{U_B\} &= \{F_B\} \end{aligned} \quad (2.16)$$

where $[K_A]$, $[K_B]$, $\{U_A\}$, $\{U_B\}$, $\{F_A\}$, $\{F_B\}$ are the stiffness matrices, displacement vectors and force vectors of bodies A and B respectively. The displacement and force vectors include the contact displacements and forces also. These equations can be combined into a single equation:

$$\begin{bmatrix} [K_A] & 0 \\ 0 & [K_B] \end{bmatrix} \begin{Bmatrix} \{U_A\} \\ \{U_B\} \end{Bmatrix} = \begin{Bmatrix} \{F_A\} \\ \{F_B\} \end{Bmatrix}$$

$$\text{or } [K] \{U\} = \{F\} \quad (2.17)$$

The equation (2.17) cannot be solved in the given form as at the contact nodes, neither the displacements nor the forces are known. To overcome this difficulty contact conditions are used.

2.3 CONTACT CONDITIONS:

There are two set of contact conditions, one on the unknown contact forces and the other on the displacements.

Let the i -th node of body A be in contact with the j -th node of body B (Fig. 2.3). Let 'n' and 's' denote the normal and tangential directions respectively at the contact node.

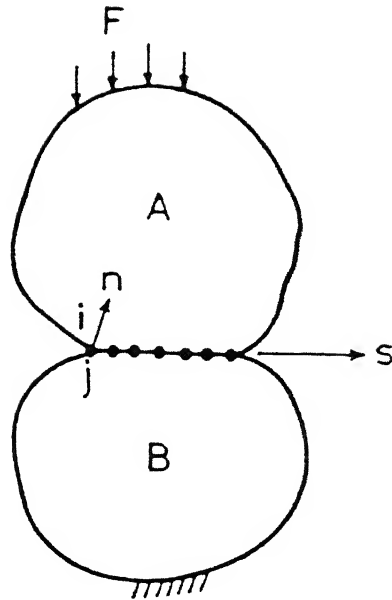


Fig.2.3 Two bodies A and B in contact.

$$\begin{bmatrix} K_{I,I} & K_{I,II} & K_{I,III} \\ K_{II,I} & K_{II,II} & K_{II,III} \\ K_{III,I} & K_{III,II} & K_{III,III} \end{bmatrix} \begin{Bmatrix} U_I \\ U_{II} \\ U_{III} \end{Bmatrix} = \begin{Bmatrix} F_I \\ F_{II} \\ F_{III} \end{Bmatrix}$$

Fig.2.4 Re-arranged matrix.

The force conditions given by Newton's third law are:

$$(F_A)_{in} = - (F_B)_{jn} \quad (2.18)$$

$$(F_A)_{is} = - (F_B)_{js} \quad (2.19)$$

The displacement compatibility conditions are

$$(U_A)_{in} = (U_B)_{jn} + \epsilon \quad (2.20)$$

$$(U_A)_{is} = (U_B)_{js} \quad (2.21)$$

where ϵ denotes the initial clearance between the nodes which come in contact.

However, the tangential displacement compatibility (2.21) is valid only when the nodes do not slip. Slip occurs when the shear force exceeds or equals the frictional resistive force. Frictional resistive force is dependent on the coefficient of friction and the normal force at the node. Therefore, if slip occurs equation (2.21) is replaced by

$$|(F_A)_{js}| = \mu |(F_A)_{jn}| \quad (2.22)$$

This condition can be applied to body B also.

In order to apply these conditions to the system of equations (2.17), they have to be expressed in terms of the 'x' and 'y' components. Resolving 'n' and 's' components along the x and y axes, we get (See Fig. 2.3).

$$\begin{aligned} (F_A)_{in} &= -(F_A)_{ix} \sin \alpha + (F_A)_{iy} \cos \alpha \\ (F_A)_{is} &= +(F_A)_{ix} \cos \alpha + (F_A)_{iy} \sin \alpha \end{aligned} \quad (2.23)$$

where ' α ' is the angle which 's'-direction makes with x-axis.

Similarly $(F_B)_{jn}$, $(F_B)_{js}$, $(U_A)_{in}$, $(U_A)_{is}$, $(U_B)_{jn}$ and $(U_B)_{js}$ can be expressed in terms of x and y components. Substituting eq.

(2.23) and similar relations in equations (2.18) - (2.22). We then get,

$$-(F_A)_{ix} \sin \alpha + (F_A)_{iy} \cos \alpha - (F_B)_{jx} \sin \alpha + (F_B)_{jy} \cos \alpha = 0 \quad (2.24)$$

$$(F_A)_{ix} \cos \alpha + (F_A)_{iy} \sin \alpha + (F_B)_{jx} \cos \alpha + (F_B)_{jy} \sin \alpha = 0 \quad (2.25)$$

$$(U_A)_{ix} \sin \alpha - (U_A)_{iy} \cos \alpha - (F_B)_{jx} \sin \alpha + (F_B)_{jy} \cos \alpha = 0 \quad (2.26)$$

$$(U_A)_{ix} \cos \alpha + (U_A)_{iy} \sin \alpha - (U_B)_{jx} \cos \alpha - (U_B)_{jy} \sin \alpha = 0 \quad (2.27)$$

$$((ss \cos \alpha + \mu \sin \alpha) (F_B)_{jx} + (ss \sin \alpha - \mu \cos \alpha) (F_B)_{jy}) = 0 \quad (2.28)$$

where ss is the sign of $(F_B)_{js}$ and sn that of $(F_B)_{jn}$. Note that Eq. (2.27) is applied for no slip condition while eq. (2.25) is to be used when there is slip.

2.4 Application of Contact Conditions:

It can be seen that corresponding to every contact pair (i, j) , there are four equations in the set (2.17). Two equations - $(2i-1)$ -th Eq. for x-direction and $(2i)$ -th for y-direction for the body A and the remaining two, $(2j-1)$ -th Eq. and $(2j)$ -th, for the body B. As stated earlier, neither the displacement associated with these nodes nor the forces (i.e. the right hand side of these equations) are known. Therefore, these equations cannot be solved as such. However, for every contact pair, there are four contact conditions. The strategy is to replace these equations with unknown right hand sides by the contact conditions which have the known right hand side. The matrix operations required for this process are described below.

First the $(2i-1)$ -th Eq. of body A is replaced by Eq. (2.24). Since $(F_A)_{ix}$ and $(F_A)_{iy}$ are equal to the left hand sides of $(2i-1)$ -th and $(2i)$ -th Eq. of body A and $(F_B)_{jx}$ and $(F_B)_{jy}$ are equal to the left hand side of $(2j-1)$ -th and $(2j)$ -th Eq. of body B, the condition states that

$$\begin{aligned} & (-\sin \alpha) (2i - 1)\text{th Eq. of body A} \\ & + (\cos \alpha) (2i)\text{-th Eq. of body A} \\ & + (-\sin \alpha) (2j-1)\text{-th Eq. of body B} \\ & + (\cos \alpha) (2j)\text{-th Eq. of body B} = 0 \end{aligned}$$

Thus after replacement, the $(2i-1)$ -th row of the $[K_A]$ becomes equal to

$$\begin{aligned} & (-\sin \alpha) (2i - 1)\text{-th row of } [K_A] \\ & + (\cos \alpha) (2i)\text{-th row of } [K_A] \\ & + (-\sin \alpha) (2j-1)\text{-th row of } [K_B] \\ & + (\cos \alpha) (2j)\text{-th row of } [K_B] \end{aligned}$$

The $(2i-1)$ -th row of $[F_A]$ is set to zero.

Next, the $(2i)$ -th Eq. of body A is replaced by the Eq. (2.25). The matrix operations for this replacement are similar. Now, the $(2i)$ -th row of $[K_A]$ is replaced by the combination of $(2i-1)$ -th and $(2i)$ -th rows of $[K_A]$ and $(2j-1)$ -th and $(2j)$ -th rows of $[K_B]$, the coefficients of the combination given by the Eq. (2.25). The $(2i)$ -th row of $[F_A]$, becomes zero. Note that the Eq. (2.25) involves the original $(2i-1)$ -th row of $[K_A]$ and not the modified one. Thus the $(2i-1)$ -th row of $[K_A]$ has to be stored before applying the first contact condition.

The third condition is applied in the end, the reason for which is explained later. The fourth contact condition, discussed

hereby, is used to replace the $(2j-1)$ -th Eq. of body B. Eq. (2.27) is used for the no slip condition. To apply this condition, the $(2j-1)$ -th row of $[K_B]$ is made zero except for the element in $(2i-1)$, $(2i)$, $(2j-1)$ and $(2j)$ columns which are respectively $\cos \alpha$, $\sin \alpha$, $(-\cos \alpha)$ and $(-\sin \alpha)$. The $(2j-1)$ -th row of $\{F_B\}$ is made zero. Thus the application of displacement contact condition is more simpler than that of force constant condition which involves certain row operations. In case of slip, Eq. (2.28) is used. This condition is similar to the first two conditions except that it involves only two equations, i.e., $(2j-1)$ -th and $(2j)$ -th equations of body B. Here, the $(2j-1)$ -th row of $[K_B]$ is replaced by the linear combination of $(2j-1)$ -th and $(2j)$ -th rows of $[K_B]$, the coefficients of the combination being given by Eq. (2.28). the $(2j-1)$ -th row of $\{F_B\}$ is then made zero.

Finally, while applying the third contact condition the $(2j)$ -th row of $[K_B]$ is made zero except the elements in the columns $(2i-1)$, $(2i)$, $(2j-1)$ and $(2j)$ which are given by $(\sin \alpha)$, $(-\cos \alpha)$, $(-\sin \alpha)$ and $(\cos \alpha)$ respectively. The $(2j)$ -th row of $\{F_B\}$ is replaced with clearance (ϵ).

In case the third contact condition is applied before the fourth, $(2j)$ -th Eq. of body B gets modified. However, for slip, the original $(2j)$ -th Eq. is required for the fourth condition. So by applying fourth earlier, we avoid storing $(2j)$ -th row of $[K_B]$.

Note that application of the contact conditions makes the coefficient matrix unsymmetric.

2.5 SUB-STRUCTURING:

An iterative scheme involving large unsymmetric matrices requires a large storage and a considerable amount of computing

time. To reduce both storage and computing time, the stiffness matrix is stored in skyline form and then decomposed to a much smaller size using sub-structuring.

The first step in substructuring is to rearrange the rows and columns of the global stiffness matrix as shown below:

$$\begin{bmatrix} K_{I,I} & K_{I,II} & K_{I,III} \\ K_{II,I} & K_{II,II} & K_{II,III} \\ K_{III,I} & K_{III,II} & K_{III,III} \end{bmatrix} \begin{Bmatrix} U_I \\ U_{II} \\ U_{III} \end{Bmatrix} = \begin{Bmatrix} F_I \\ F_{II} \\ F_{III} \end{Bmatrix} \quad (2.29)$$

Here the suffix I denotes the degrees of freedom associated with the contact nodes and the nodes at which non-zero forces are specified, II denotes the degree of freedom associated with the free surface and the internal nodes, while III denotes the degree of freedom associated with the nodes at which displacements are specified. If the prescribed displacements are zero then

$$U_{III} = 0$$

$$F_{II} = 0$$

Then the equation (2.29) reduces to

$$\begin{aligned} K_{I,I} U_I + K_{I,II} U_{II} &= F_I \\ K_{II,I} U_I + K_{II,II} U_{II} &= 0 \end{aligned} \quad (2.30)$$

Eliminating U_{II} from the above equations we get

$$\overline{K}_{I,I} U_I = F_I \quad (2.31)$$

where

$$\overline{K_{I,I}} = (K_{I,I} - K_{I,II} K_{II,II}^{-1} K_{II,I}) \quad (2.32)$$

To obtain the matrix $\overline{K_{I,I}}$, first $K_{I,I}$ is extracted in full form from the global stiffness matrices of bodies A and B in skyline form. Next $K_{II,II}$ is obtained in skyline form from the global stiffness matrices. Then $(K_{II,II}^{-1} K_{II,I})$ is obtained column-wise. If $\{C\}_i$ is its i -th column, then it can be found by solving the system

$$[K_{II,II}] \{C\}_i = \{K_{II,I}\}_{i\text{-th column}}$$

Thus the inverse of $K_{II,II}$ is not explicitly found. Then the elements of the matrix $K_{I,II} K_{II,II}^{-1} K_{II,I}$ are obtained by multiplying the rows of $K_{I,II}$ with the appropriate column of $K_{II,II}^{-1} K_{II,I}$. In the last two steps, the rows of $K_{I,II}$ or the columns of $K_{II,I}$ are generated from the skyline form as and when required. Finally $\overline{K_{I,I}}$ is obtained using Eq. (2.32).

Substituting this leads to a very small set of equations (2.31) which is solved after applying the contact conditions. Displacements U_{II} are obtained by back substituting U_I in the equation

$$U_{II} = -K_{II,II}^{-1} K_{II,I} U_I \quad (2.33)$$

Once all the displacements are known F_I can be readily found using the third set of Eq. (2.29).

2.6 Program Algorithm

The set of equations (2.31) are solved iteratively by applying the contact conditions in the following way.

1. A set of nodal points is assumed to be in contact (it should

include all possible contact points) and equations (2.31) are solved after applying the contact conditions for no slip.

2. The sign of the normal force at each node in the contact zone is checked. The normal nodal forces cannot be tensile. Hence all those nodes where the normal force turns out to be tensile are deleted from the possible contact zone in the next iteration.

3. The ratio of shear force to normal force at each node in the contact zone is checked. Slipping occurs when the nodal shear force exceeds or equals the product of nodal normal force and the coefficient of friction. For the nodes which slip, the condition (2.26) is replaced by eq. (2.27) in the next iteration.

4. Equation (2.31) are solved by repeating steps 2 and 3 until all the normal nodal forces in the contact zone come out to be compressive and the ratio of the shear force to the normal force for all the nodes in the contact zone becomes either equal to or less than the coefficient of friction.

2.7 EVALUATION OF STRESSES:

To evaluate the stress components at a point, first the nodal displacement vector $\{u\}_{\text{nodal}}^e$ of the element to which the point belongs is extracted from the solution vector $\{U\}$. Stresses are then calculated using the Eqs. (2.5) and 2.12) i.e.

$$\{\sigma\} = [D] \{B\} \{u\}_{\text{nodal}}^e \quad (2.34)$$

Here we need stresses in the contact region which is the common boundary between bodies A and B. Normally the approximation chosen for the displacement vector (eq. 2.11) is such that the stresses do not become continuous across the inter element boundaries. Thus the stress components at a point on the

contact surface will have different values when it is considered as a point belonging to body A first and then to body later. Therefore we adopt the following procedure on the contact surface. First we choose a set of points which are different from the contact nodes. The stress components σ_x , σ_y and τ_{xy} at these points are determined using the relation (2.34) by assuming that they belong to body A first and then to body B later. Next the X-Y components of the stress vector on the contact surface are calculated using the relation

$$\begin{Bmatrix} f_x \\ f_y \end{Bmatrix} = \begin{bmatrix} \sigma_x & \tau_{xy} \\ \tau_{xy} & \sigma_y \end{bmatrix} \begin{Bmatrix} n_x \\ n_y \end{Bmatrix} \quad (2.35)$$

where n_x and n_y are the components of the unit vector along normal direction n with respect to xy axes. Then, normal and shear component of the stress vector are given by

$$\begin{aligned} f_n &= f_x n_x + f_y n_y \\ f_s &= f_x s_x + f_y s_y \end{aligned} \quad (2.36)$$

where s_x and s_y are the components of the unit vector along the tangential directions with respect to xy axes.

Finally, the magnitudes of the normal and shear components of the stress vector $\{f_s\}$ are averaged over the bodies A and B to give the contact stresses.

It may be noted that the maximum tensile stress for the planer bed-carriage problem is directly determined by using the relation (2.34), where $\{u\}_{nodal}^e$ is derived for the bottom centre element of the carriage from the solution vector $\{U\}$.

CHAPTER III

RESULTS AND DISCUSSIONS

In this chapter, first the problem of flat plate over flat plate for which the solution is known is solved to verify the applicability of the program. Then the problem of V-slide of a planer bed-carriage is considered. All the materials are assumed to be isotropic and linearly elastic. Body forces are neglected and axial thickness 'h' is taken as unity. In both the problems, four noded isoparametric element is used. The program developed is in general for unsymmetric problems, however the simplifications arising out of symmetry have been considered.

3.1 FLAT PLATE OVER A FLAT PLATE

Contact between two cast iron plates of same material with a point load at the mid-length on the top plate is analysed here. The configuration is shown in Figure 3.1(a).

For the finite element mesh, body 'A' is divided into 60 elements with 84 nodes and body 'B' is divided into 96 elements with 125 nodes. One half of this is shown in Figure 3.1(b).

For computation the following data is used:

Force at the middle,	$P = 1960 \text{ N/mm}$
Young's Modulus,	$E = 0.931 \times 10^5 \text{ N/mm}^2$
Poisson's ratio,	$\nu = 0.25$
Coefficient of friction	$\mu = 0.002, 0.20, 0.40$

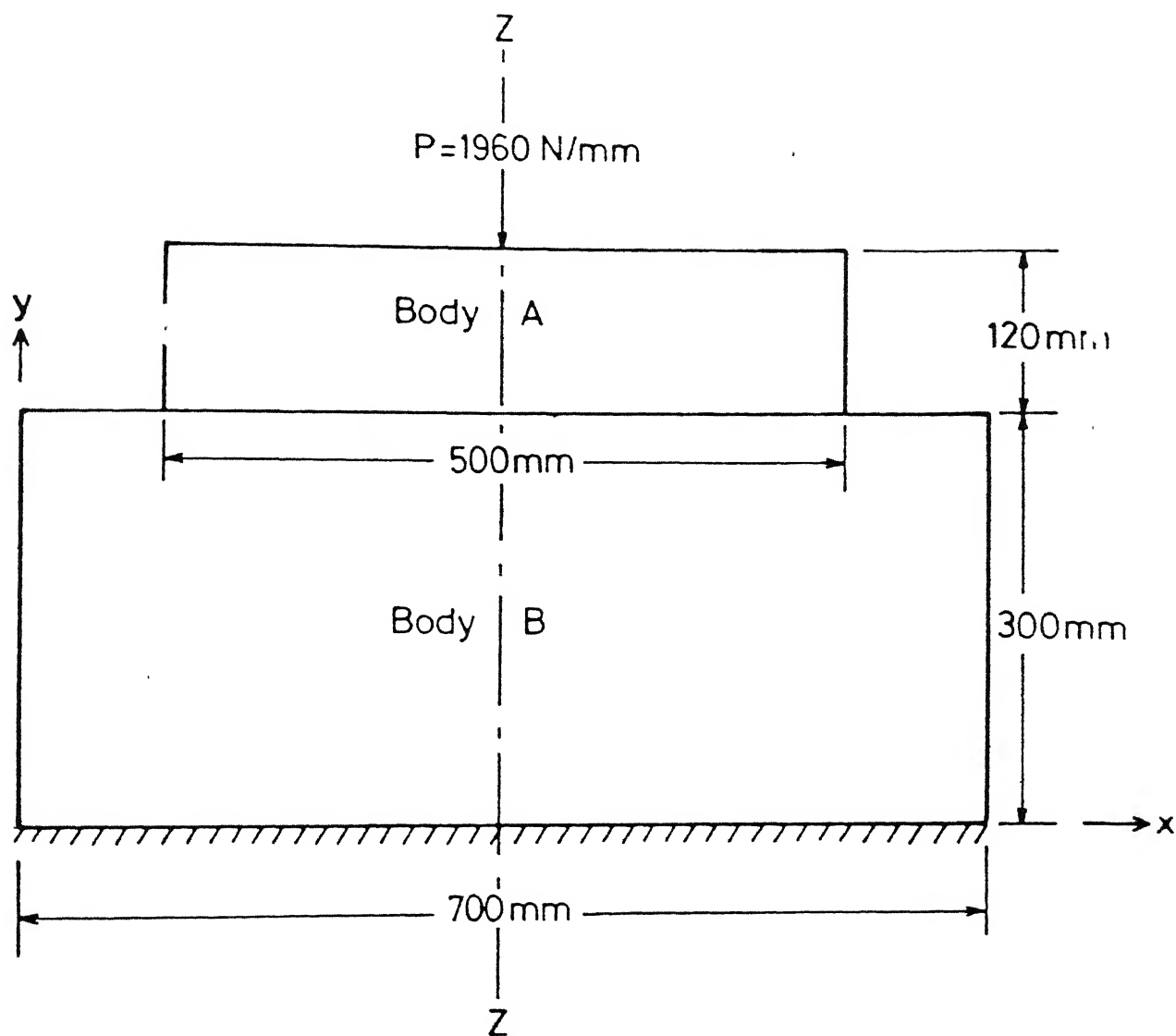


Fig.3-1(a) Flat plate over a flat plate configuration.

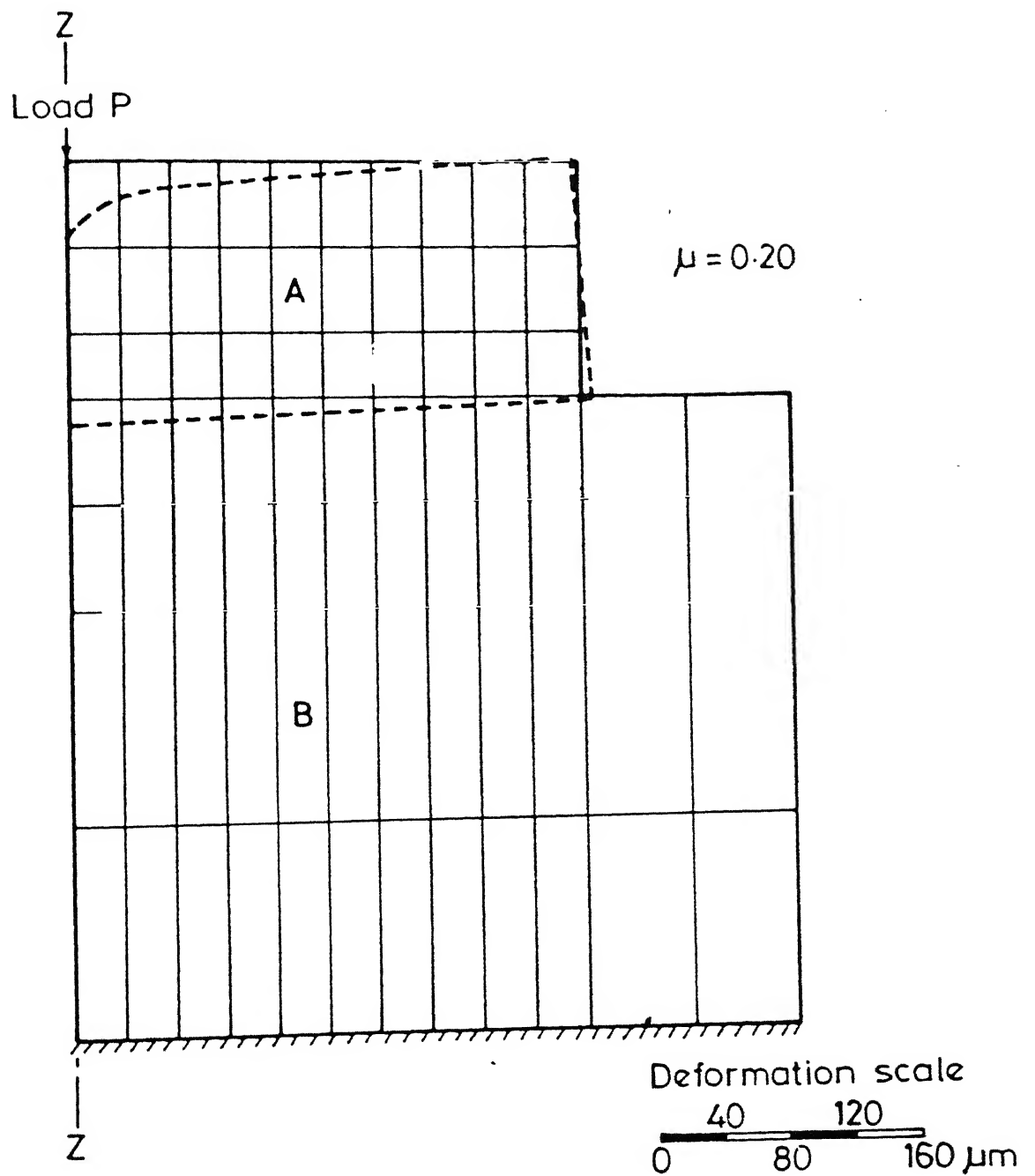


Fig.3.1(b) One half of the finite element mesh and deformed shape.

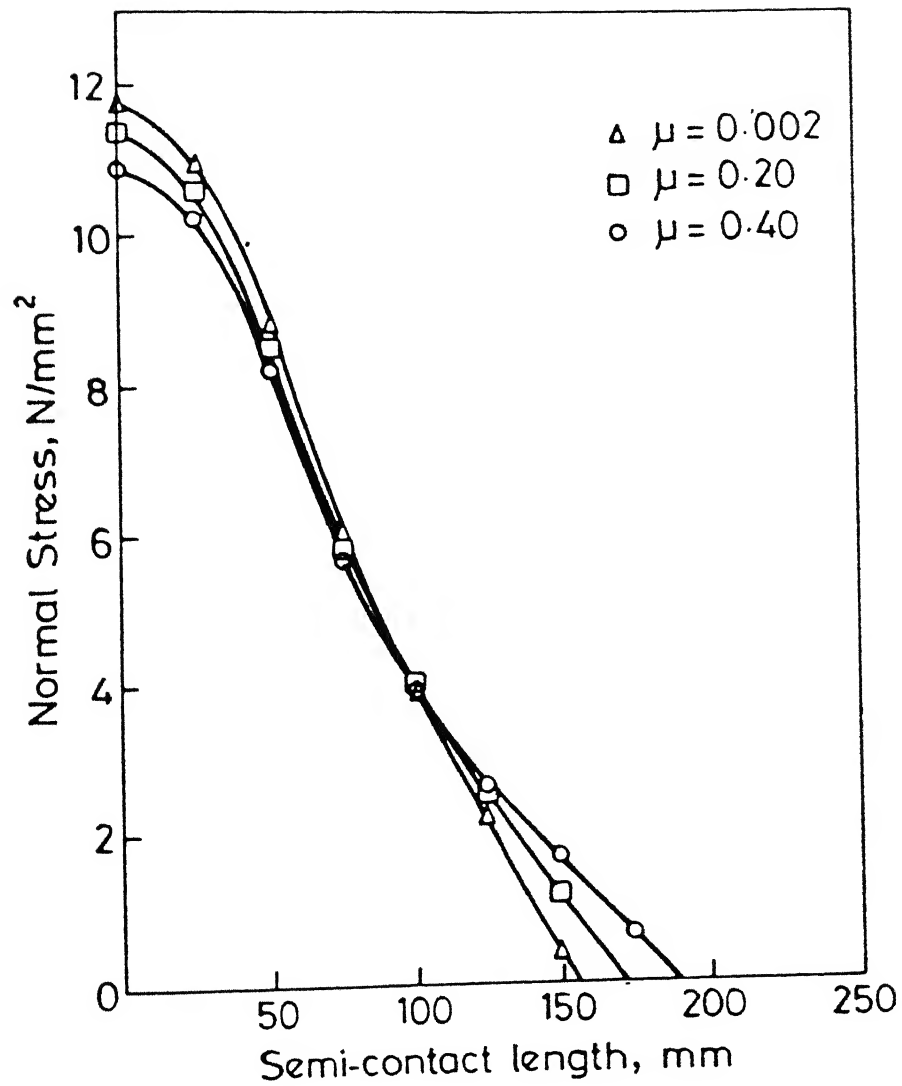


Fig.3-1(c) Variation of normal stress along the contact length for various values of μ .

To begin with 21 nodes are initially assumed to be in contact. In the converged solution only 13 nodes are found to be in contact for $\mu = 0.002$ and $\mu = 0.20$. For $\mu = 0.40$ the contact length extended to 15 nodes.

The deformed shape of the two bodies in contact for $\mu = 0.20$ is shown to an enlarged scale in Figure 3.1(b). The normal pressure distribution for various values of μ is shown in Fig. 3.1(c). It is found that the contact zone increases with increase in the value of the coefficient of friction and the maximum normal pressure decreases with increase in friction. However, the magnitude of this reduction is not very prominent. This may be due to the fact that the point of maximum pressure is under the direct influence of the applied load.

The results obtained are found to conform very closely with that of Ramesh [13]. The results of Sachdeva and Ramakrishnan [12] were validated by Ramesh [13] who had solved the same problem.

3.2 PLANAR BED - CARRIAGE CONTACT PROBLEM

A planer has a moving carriage which slides in V-shaped slidway of the bed. The cross-section of the carriage-bed configuration is shown in Figure 3.2(a). The bed and carriage dimensions were obtained from the machine no. 31, Central Workshop, IIT, Kanpur. The vertical cutting force data has been used from the reference [14] which takes into account the heavy and rough machining conditions encountered in planing. The force location has been varied from point (1) to (4) (Refer Figure 3.2 (b)). Since the structure is symmetric in geometry and loading

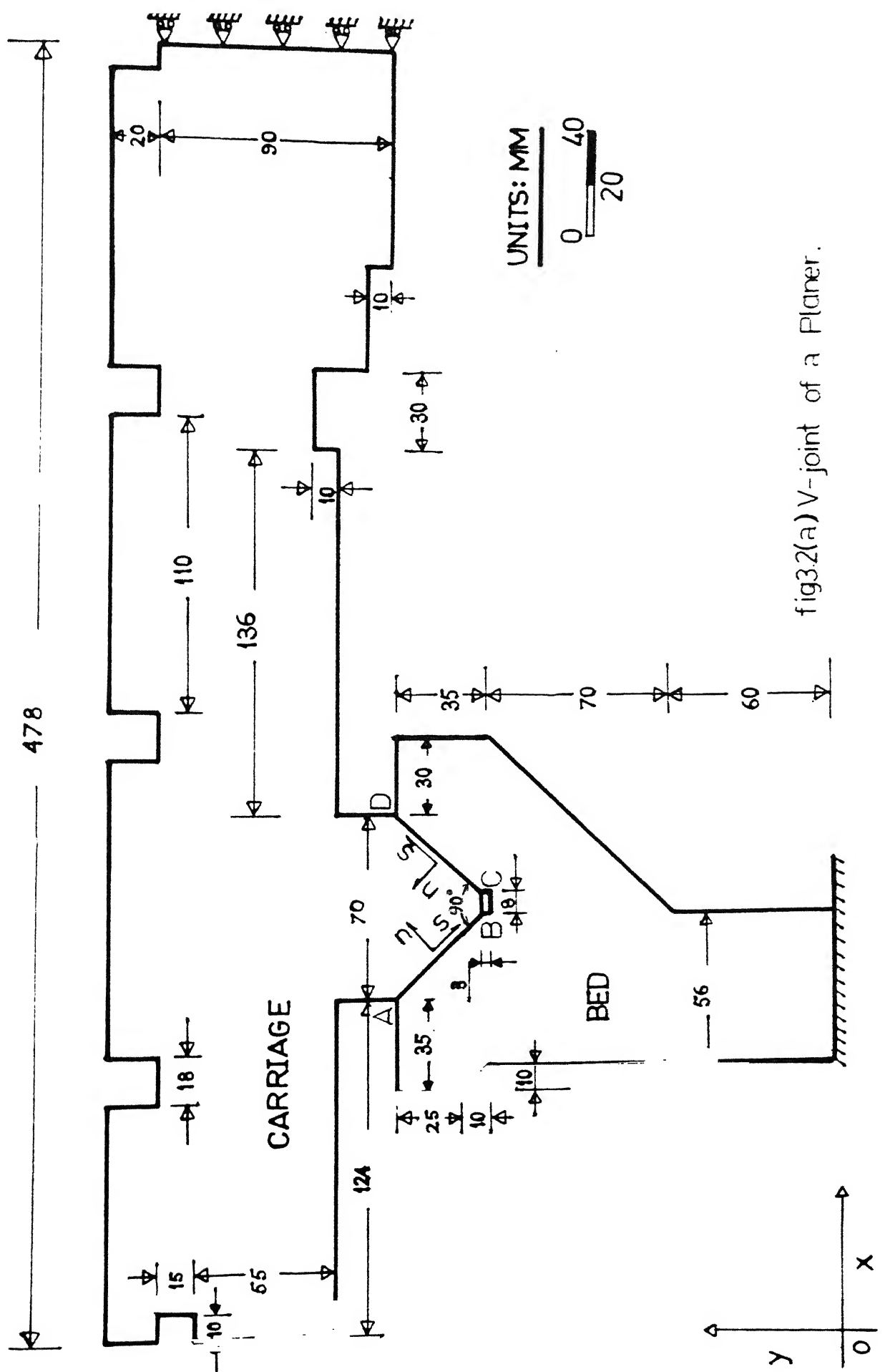


fig3.2(a) V-joint of a Planer.

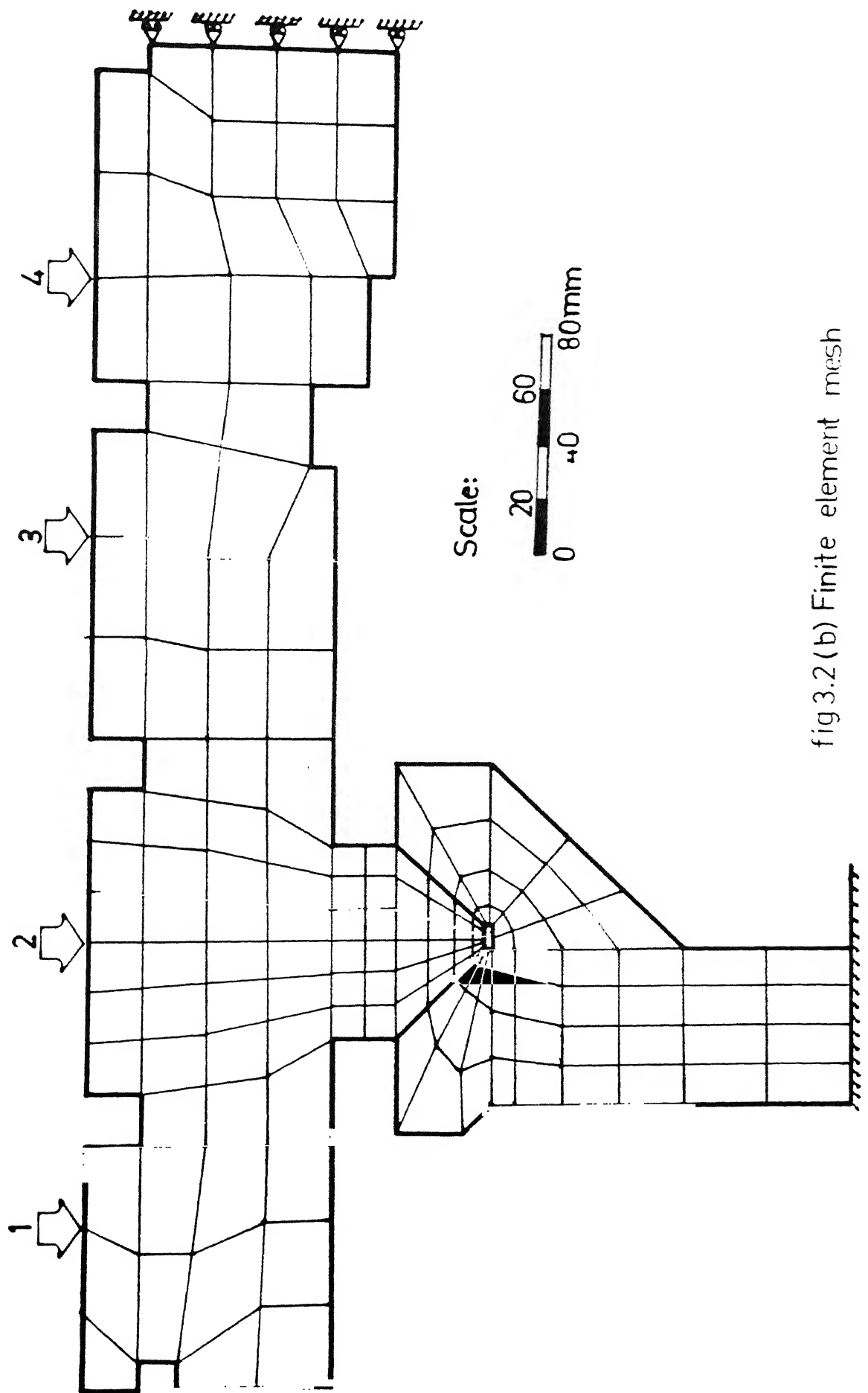


fig 3.2 (b) Finite element mesh

conditions, only half the cross-section is analysed. The symmetry conditions have been accounted by imposing u-displacements and shear stress equal to zero in the centre plane. Each case has been analysed for three values of friction accounting for the dry and boundary lubrication conditions.

The joint and the maximum structural deflections, contact length, the normal and shear contact stresses and the maximum tensile stress in the structure, have been determined to study how far the strength and deflection criteria of safe design have been incorporated.

The finite element mesh is shown in figure 3.2(b). Carriage has been divided into 103 elements with 145 nodes while the bed has been divided into 56 elements with 75 nodes. Since the bed and carriage are made of cast iron, the following properties are used:

Vertical force,	$P = 300 \text{ N/mm}$
Young's Modulus,	$E = 0.931 \times 10^5 \text{ N/mm}^2$
Poisson's ratio,	$\nu = 0.25$
Coefficient of friction,	$\mu = 0.002, 0.20, 0.40$
Strength in compression,	$\sigma_{cu} = 500 \text{ N/mm}^2$
Strength in tension,	$\sigma_{tu} = 165 \text{ N/mm}^2$
Strength in shear,	$\sigma_{su} = 50 \text{ N/mm}^2$

The general deformation pattern of the structure is shown in Figure 3.3. It corresponds to the force location at point (4). Variation of the normal deflections along the contact length for various values of μ and force locations is shown in Figure 3.4. The corresponding tangential deflections for the bed and the carriage are shown in figures (3.5) and (3.6) respectively. The

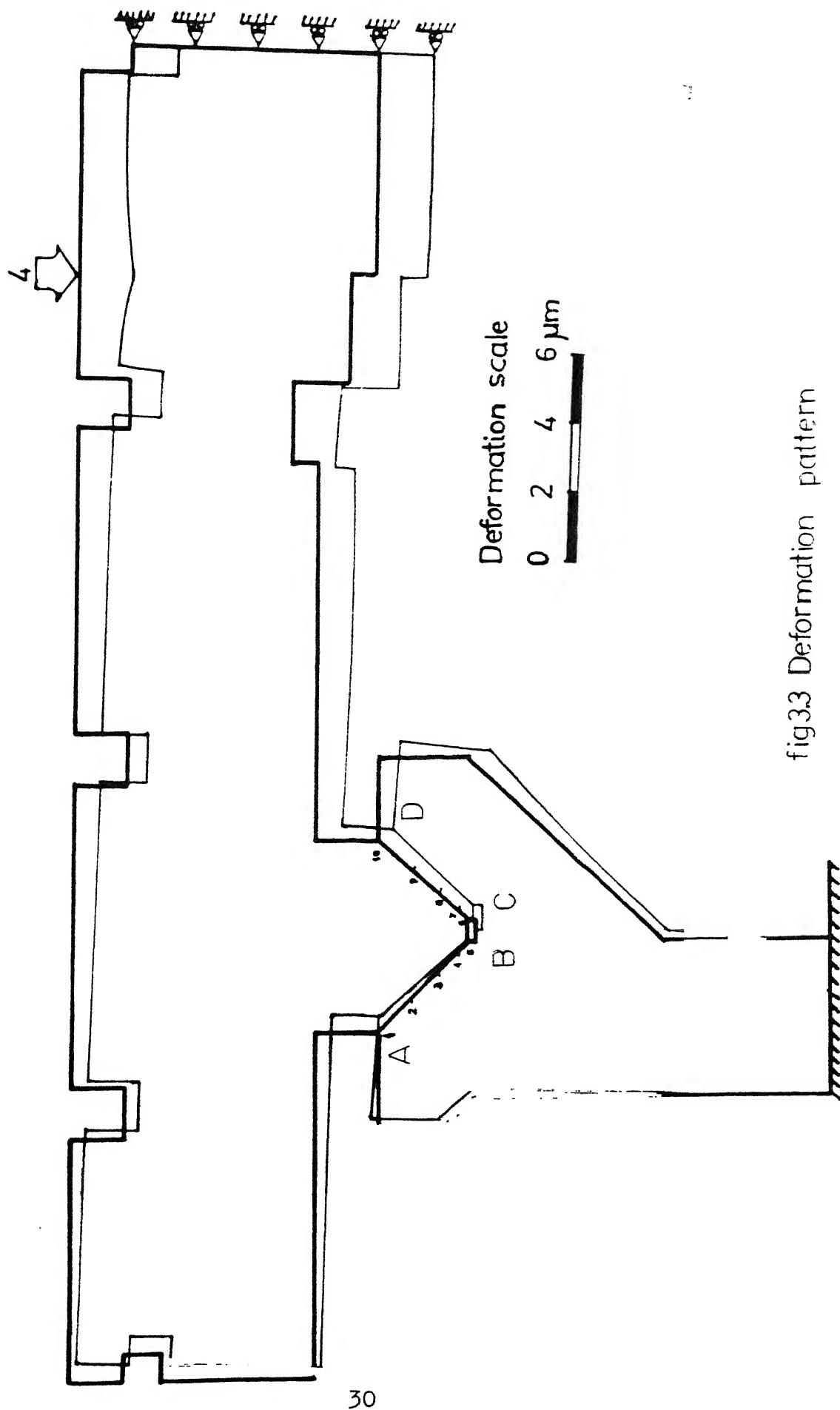


fig33 Deformation pattern

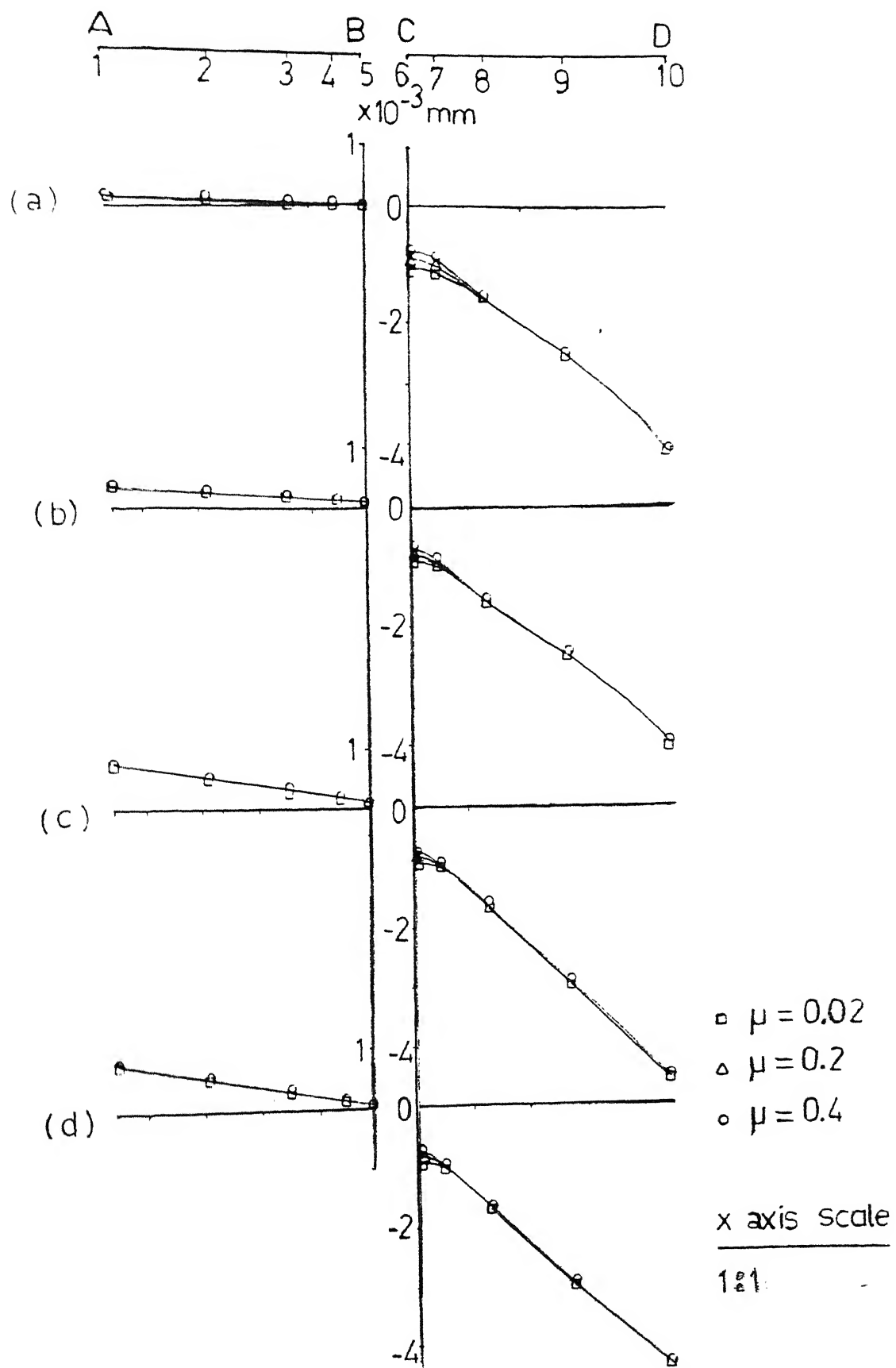


fig.3.4 Variation of normal displacements along the contact length for various values of μ

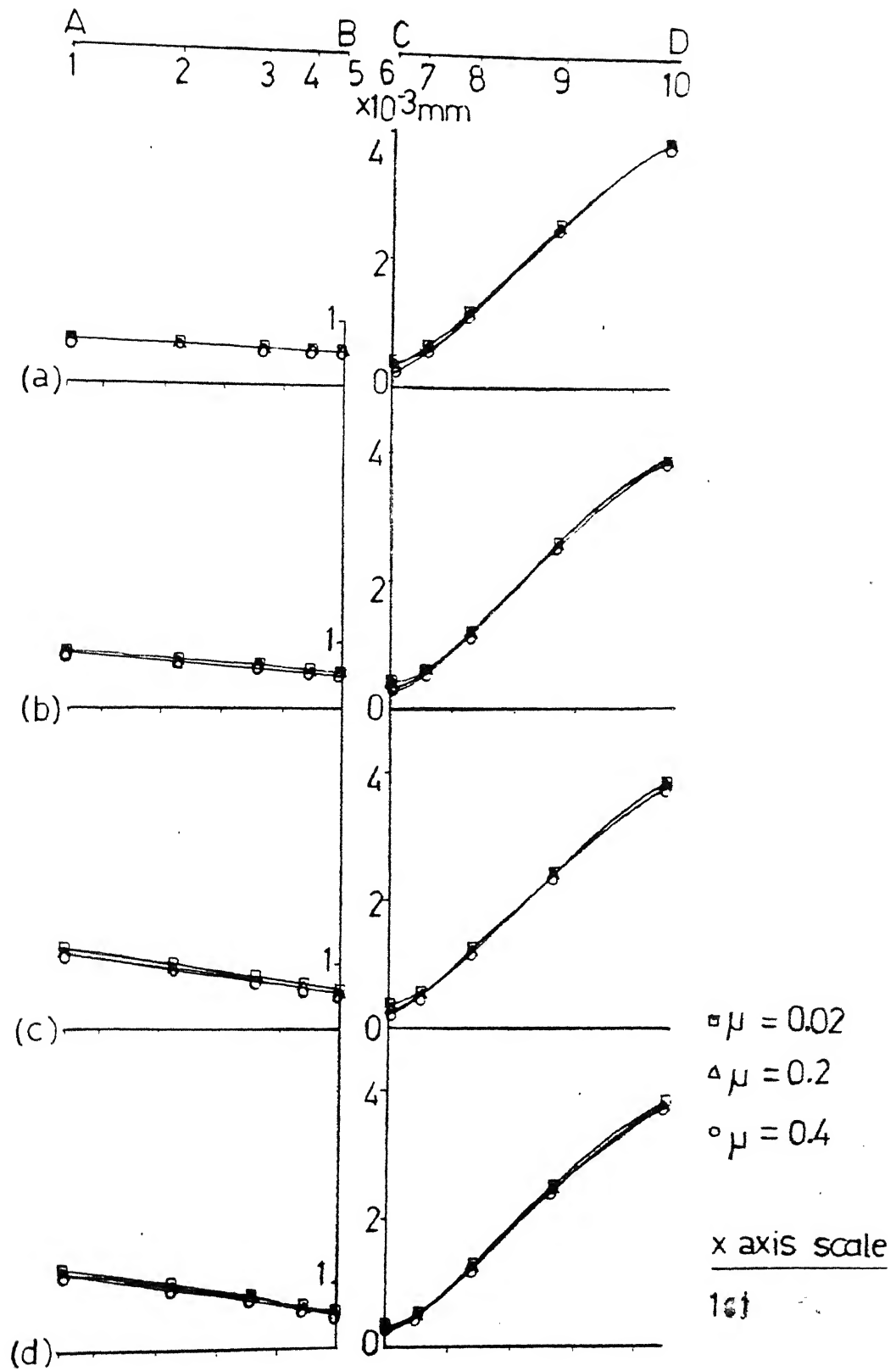


fig.3.5 Variation of tangential displacements of bed along the contact length for various values of μ

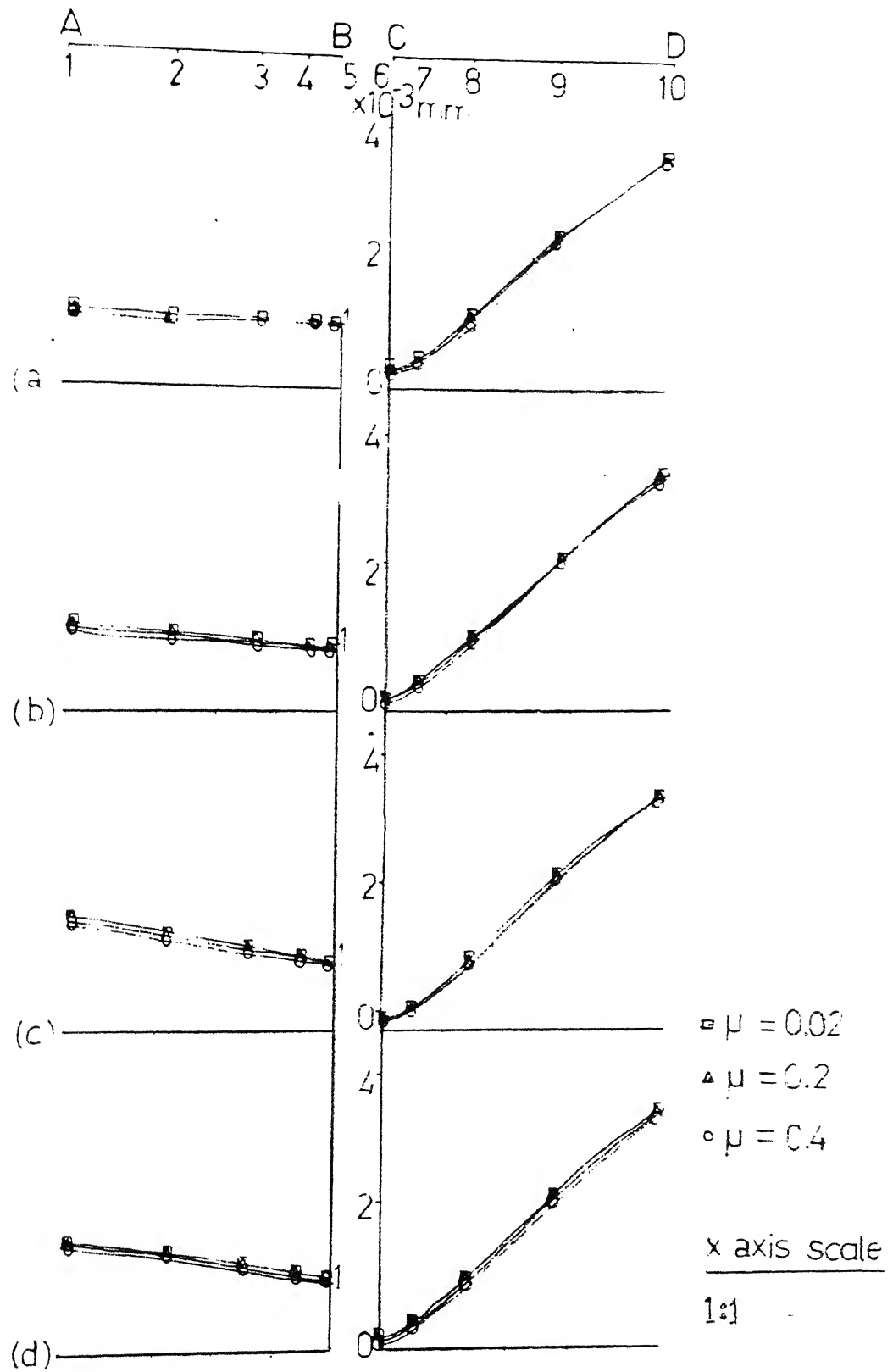


fig.3.6 Variation of tangential displacements of carriage along the contact length for various values of μ

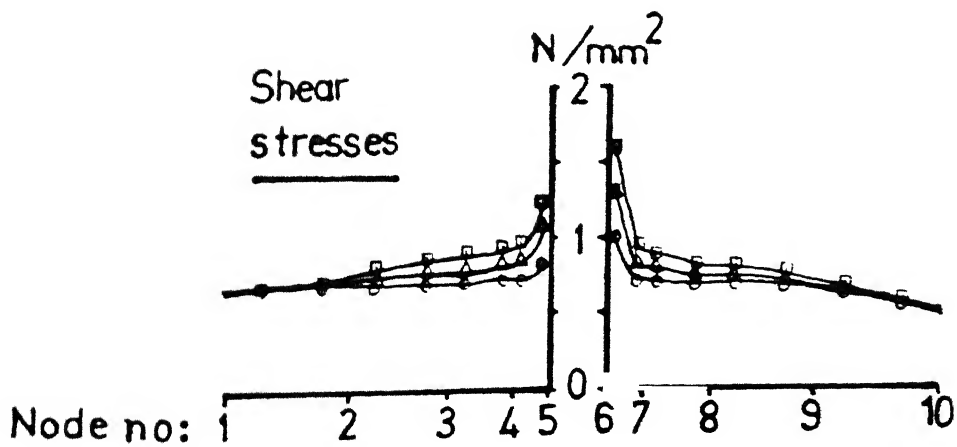
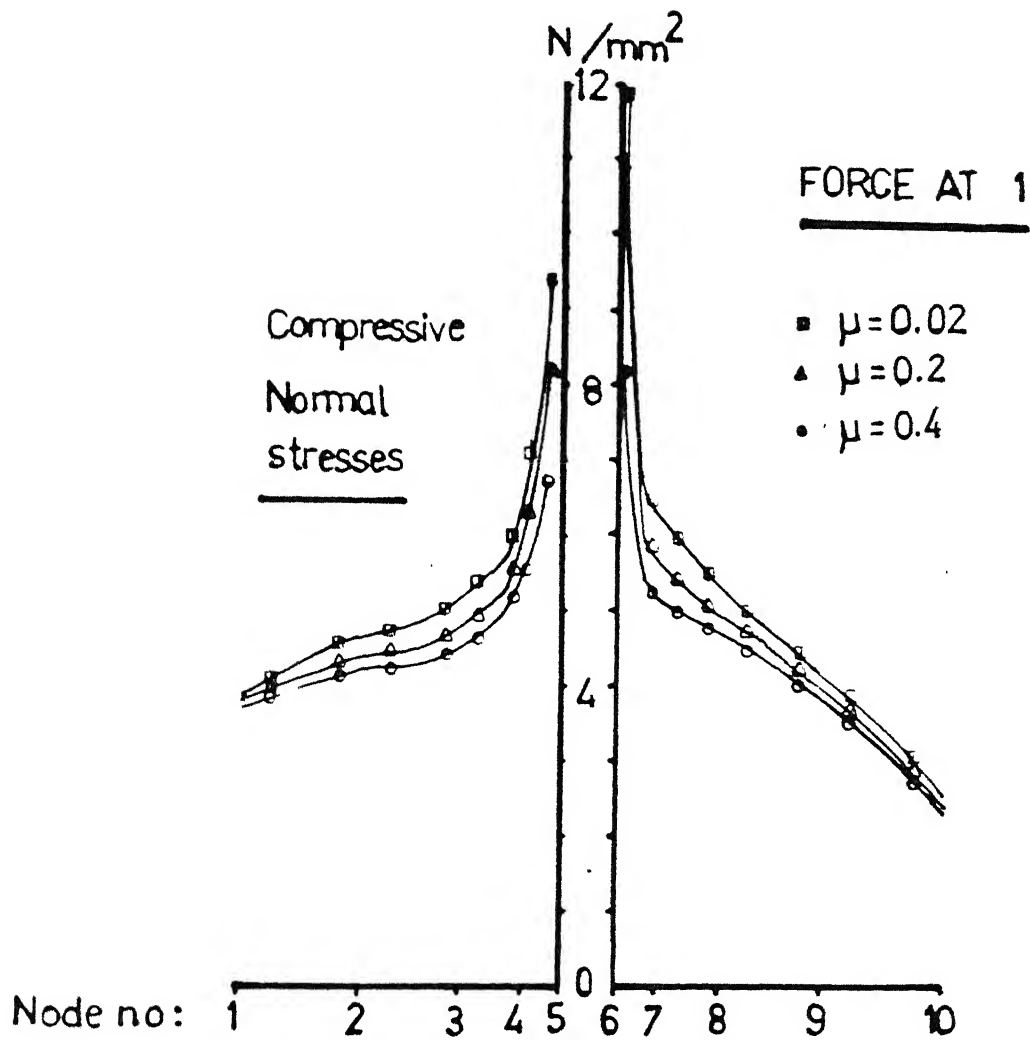


fig.37(a) Variation of normal and shear stresses along the contact length for various values of μ

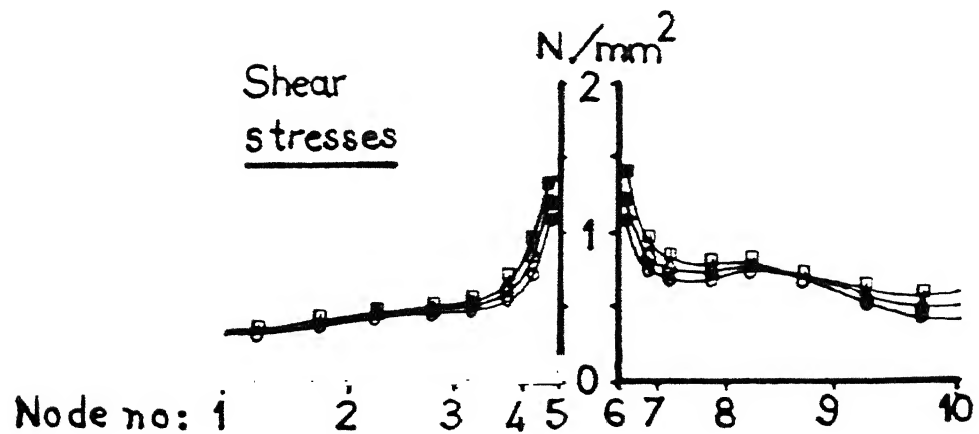
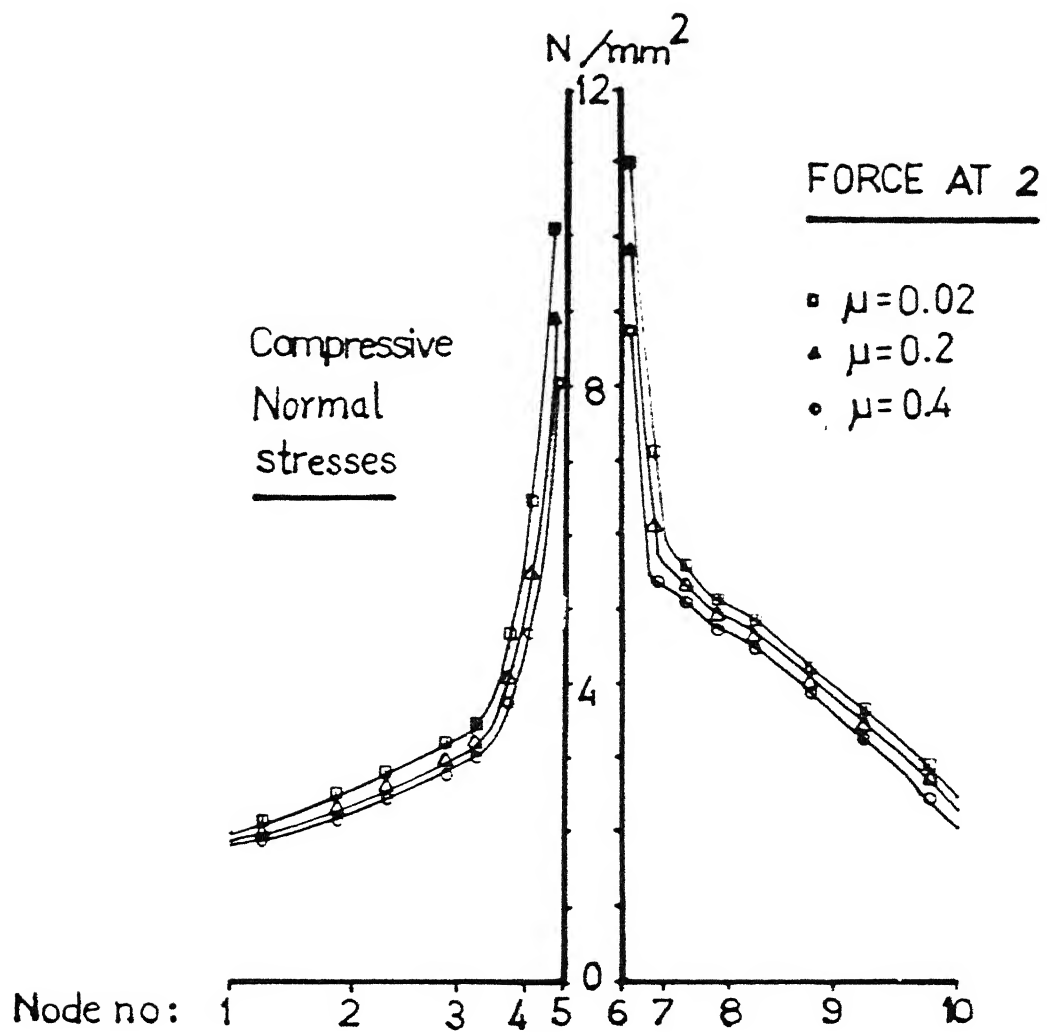


fig.3.7(b) Variation of normal and shear stresses along the contact length for various values of μ

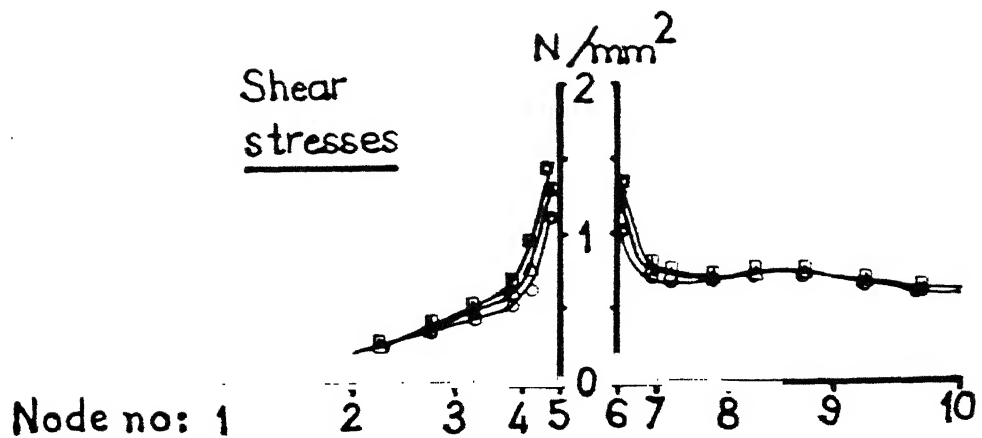
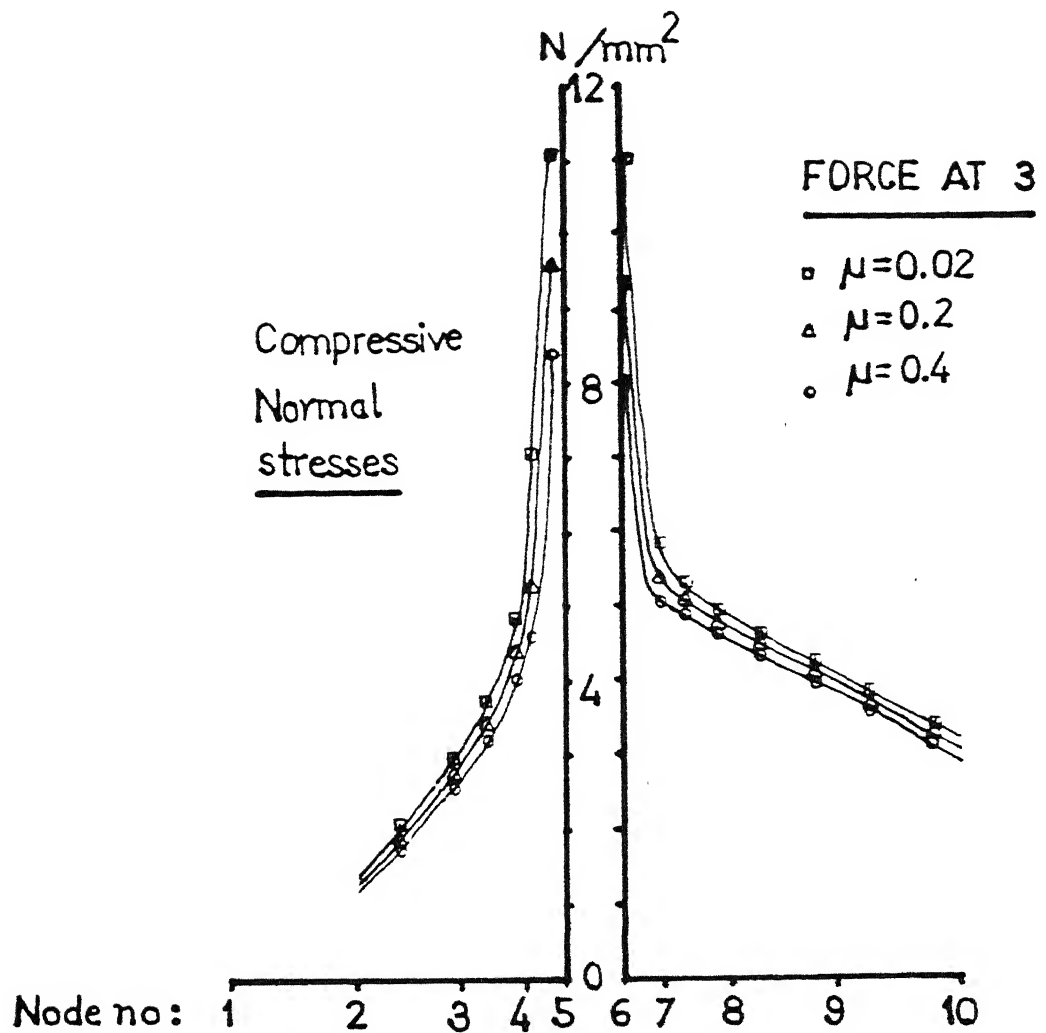


fig.3.7(c) Variation of normal and shear stresses along the contact length for various values of μ

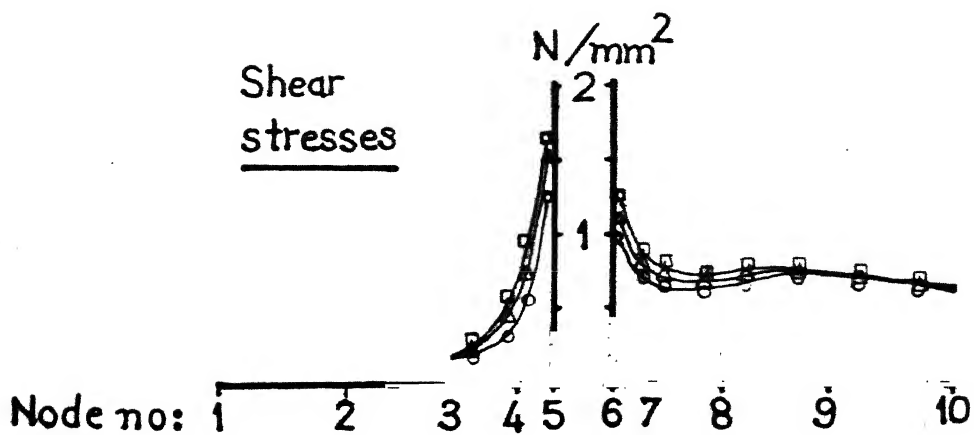
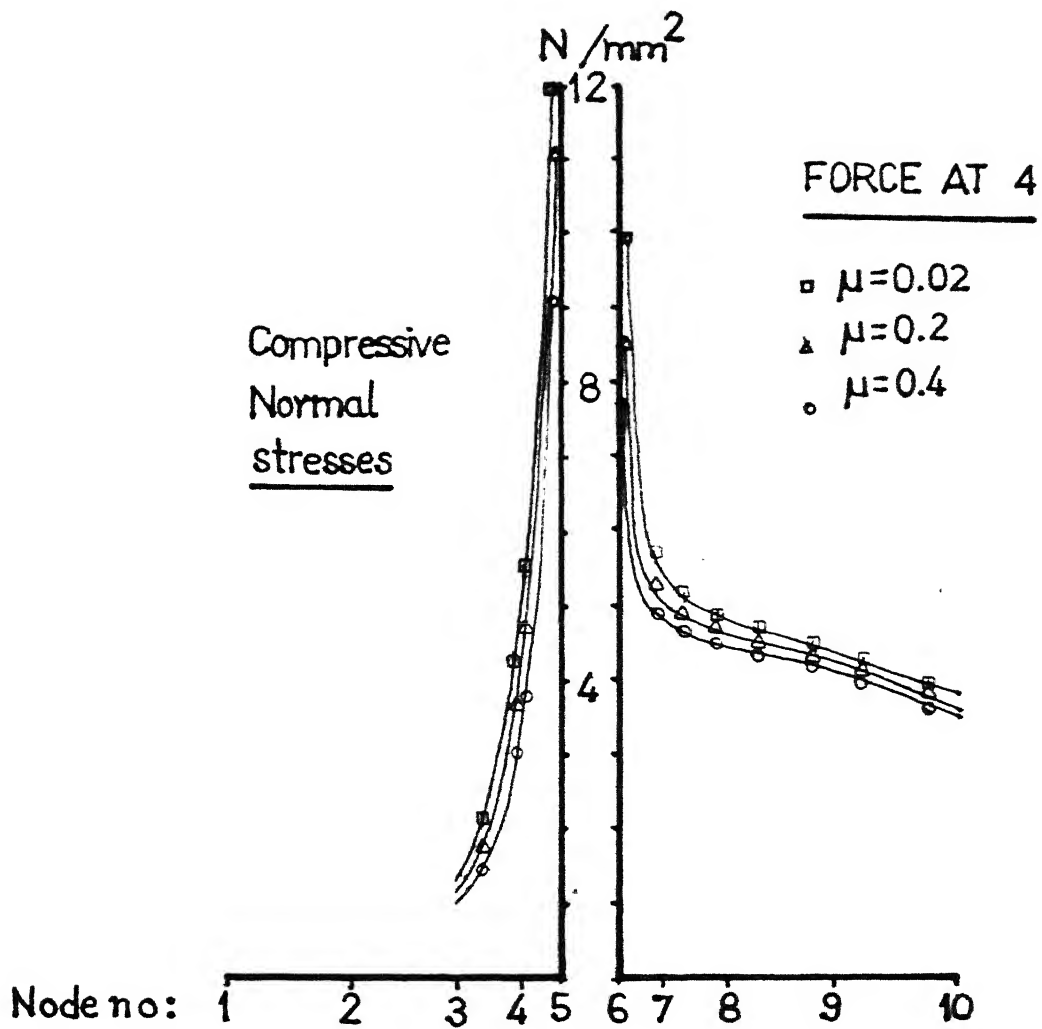


fig.3.7(d) Variation of normal and shear stresses along the contact length for various values of μ

variation of the magnitude of normal and shear stresses along the contact length for various values of μ are shown in figures 3.7(a), 3.7(b), 3.7(c) and 3.7(d) for four different locations of the applied force. For the carriage shear stresses on both the parts AB and CD act downwards. Then for the bed, they will be in the upwards direction.

The observations for the four force locations are as follows:

Case 1: Force at location (1).

All the nodes slip initially but remain in contact till convergence. The solution converges in three iterations. The bottom centre node of the carriage deflects down vertically by $0.72 \mu\text{m}$. The tensile stress in the neighbourhood of this point is -2.3 N/mm^2 .

The salient data for the contact zone is given in Table A.

Table A: Case (1) Data

Value of μ	Node No.	Max. Normal def. $\times 10^{-2}$ (mm)	Node No.	Max. Tang. def. $\times 10^{-2}$ (mm)	Node No.	Max. Compr. stress (N/mm ²)	Node No.	Max. Shear stress (N/mm ²)
0.02	10	0.435	10	0.384	6	12.0	6	1.6
0.2	10	0.431	10	0.382	6	11.0	6	1.3
0.4	10	0.431	10	0.382	6	8.2	6	1.0

Case 2: Force at location (2)

All the nodes slip initially but remain in contact till convergence. The solution converges in three iterations. The bottom centre node of the carriage deflects down vertically by $0.83 \mu\text{m}$. The tensile stress in the neighbourhood of this point is -0.7 N/mm^2 .

The salient data for the contact zone is given in Table B.

Table B: Case (2) Data

Value of μ	Node No.	Max. Normal def. $\times 10^{-2}$ (mm)	Node No.	Max. Tang. def. $\times 10^{-2}$ (mm)	Node No.	Max. Compr. stress (N/mm ²)	Node No.	Max. Shear stress (N/mm ²)
0.02	10	0.436	10	0.384	6	11.0	6	1.4
0.2	10	0.435	10	0.383	6	9.8	6	1.2
0.4	10	0.435	10	0.381	6	8.6	6	1.1

Case 3: Force at location (3).

All the nodes slip initially and node 1 goes out of contact before convergence. The solution converges in four iterations. The bottom centre node of the carriage deflects down vertically by 1.55 μm . the tensile stress in the neighbourhood of this point is 31.3 N/mm².

The salient data for the contact zone is given in Table C.

Table C: Case (3) Data.

Value of μ	Node No.	Max. Normal def. $\times 10^{-2}$ (mm)	Node No.	Max. Tang. def. $\times 10^{-2}$ (mm)	Node No.	Max. Compr. stress (N/mm ²)	Node No.	Max. Shear stress (N/mm ²)
0.02	10	0.440	10	0.385	5	11.0	5	1.4
0.2	10	0.439	10	0.384	5	9.6	5	1.3
0.4	10	0.439	10	0.383	5	8.3	5	1.1

Case 4: Force at location (4).

All the nodes slip initially and nodes 1 and 2 go out of contact before convergence. The solution converges in four

iterations. The bottom centre node of the carriage deflects down vertically by $1.59 \mu\text{m}$. the tensile stress in the neighbourhood of this point is 48.7 N/mm^2 .

The salient data for the contact zone is given in Table D.

Table D: Case (4) Data.

Value of μ	Node No.	Max. Normal def. $\times 10^{-2}$ (mm)	Node No.	Max. Tang. def. $\times 10^{-2}$ (mm)	Node No.	Max. Compr. stress (N/mm^2)	Node No.	Max. Shear stress (N/mm^2)
0.02	10	0.41	10	0.386	5	12.0	5	1.6
0.2	10	0.440	10	0.385	5	11.0	5	1.3
0.4	10	0.440	10	0.384	5	9.0	5	1.2

The study of normal deflections (See Figure 3.4) indicates that the normal deflections are high at the outer edge of the V-joint. On the side CD, their magnitude is higher and they rise more rapidly. Change in friction affects the normal deflections only over a small portion of the side CD. The deflections are found to reduce slightly with increase in μ . As the force is moved from location (1) to (4), the maximum value of normal deflection increases on both sides.

The study of tangential deflection (See Figures 3.5 and 3.6) gives the information about the relative slipping between the two bodies. On side AB, it is the carriage which slips relative to the bed and that too in the downward direction, whereas on side CD, it is the bed which slips and it is in upward direction. The values of tangential deflection decrease marginally as μ is

increased, almost uniformly over both the sides of the contact region.

For case (1) (Figure 3.7(a)), it is seen that the maximum compressive stress is taken by node 6. Node 5 experiences less compressive stress. This difference gets reduced when the force is at location (2) (Figure 3.7(b)). At location (3) (Figure 3.7(c)), the peak compressive stresses at nodes 5 and 6 become almost equal whereas at location (4) (Figure 3.7(d)), the maximum stress shifts to node 5. Stresses at other nodes on side AB reduce progressively when the force moves from location (1) to (4). The shear stresses show a trend similar to that of the normal stresses. In each case it has been observed that with the increase in μ , the peak stress falls and the stress curves tend to flatten.

CHAPTER IV

CONCLUSIONS AND SUGGESTIONS FOR FUTURE WORK

4.1 CONCLUSIONS:

The following conclusions can be drawn from the study of the planer bed-carriage contact problem.

1. The method developed can be used to analyse any complex geometry, including unsymmetric geometry. As it uses substructuring technique, it can be used to solve very large problems. Very few iterations are required for convergence. The method can account for extremely low or high values of friction.
2. Stresses in the carriage are very much less than the ultimate values but probably strength is not the criterion used for designing a carriage, it is the deflection, which affects the machining accuracy.
3. Shear stresses which contribute to wear have been found to be larger at the bottom of the V joint. Differential use of costlier material or case carburising of such areas can extend the useful life of the machine.
4. Stress concentration has been observed at the sharp corners of the joint.
5. The maximum deflection observed seems to be within the acceptable machining accuracy level. However, stiffness members between the two V-slides of the bed may help in further improving the machining accuracy.

4.2 SUGGESTIONS FOR FUTURE WORK

- (i) The method can easily take care of variable coefficient of friction. However, experimental data is lacking for use in the study of contact problems.
- (ii) The method can be extended to tackle 3-D problems so that the problem of V-slide of a planer bed-carriage can be analysed more realistically.
- (iii) Multiple contact problems can be studied.
- (iv) The method presented can be modified for incremental loading by increasing the force from a low value to the required maximum in several steps. At each load step, it may be determined whether a node slips or adheres and appropriate contact conditions may thus be applied progressively.
- (v) Higher order elements can be used for better results.

REFERENCE

- [1] N. Back, M. Burdekin and A. Cowley, Pressure Distributions and Deformations of Machined Components in Contact, *Int. J. Mech. Sci.*, 15, 993-1010 (1973).
- [2] H. Hertz, On the contact of Elastic Solids, *J. of Math.*, 92, 156-171 (1882) (in German). *Misc. Papers (in English)* by H. Hertz, Jones and Schott, Macmillan London (1896).
- [3] N.I. Muskhelishvili, Some Basic Problems of the Mathematical Theory of Elasticity, Nordhoff, The Netherlands, (1963).
- [4] G.M.L. Gladwell, Contact Problems in the classical Theory of Elasticity, Sijthoff and Nordhoff, The Netherlands, (1973).
- [5] S.K. Chan and I.S. Tuba, A finite Element Method for contact Problems of Solid Bodies - Part I. Theory and Validation. *Int. J. Mech. Sci.*, 13, 615-625 (1971).
- [6] S. Ohte, Finite Element Analysis of Elastic Contact Problems, *Bulletin of JSME*, 16, 95, 797-804 (1973).
- [7] A. Francavilla and O.C. Zienkiwicz, A Note on the Numerical Computation of Elastic Contact Problems, *Int. J. Num. Meth. Engg.*, 14, 337-357 (1979).
- [8] N.D. Hung and G. Sauxe, Frictionless Contact of Elastic Bodies by Finite Element Method and Mathematical Programming Techniques, *Computers and Struct.*, 11, 55-67 (1980).
- [9] T.D. Sachdeva, C.V. Ramakrishnan and R. Natrajan, A Finite Element Method for the Elastic Contact Problems with Friction, *J. of Appl. Mech.*, 103, 456-461 (1981).
- [10] T.D. Sachdeva and C.V. Ramakrishnan, A Finite Element Solution for the two Dimensional Elastic Contact Problems with Friction, *Int. J. Num. Meth. Engg.*, 17, 1257-1271 (1981).
- [11] Torstenfelt, Contact Problems with Friction in General Purpose Finite Element Computer Programs, *Computers and Struct.*, 16, 487 (1983).
- [12] P.V. Kishore, Solution Method to Contact Problems Minimization of Dissipation Energy Approach, M. Tech. Thesis, Mech. Engg. Dept., I.I.T. Kanpur (1988).
- [13] M.D. Ramesh, Finite Element Analysis of a Machine Tool Joint as a Contact Problem, M. Tech., Thesis, Mech. Engg. Dept., IIT Kanpur (1988).
- [14] B.L. Juneja and G.S. Sekhon, Fundamentals of Metal Cutting and Machine Tools, Wiley Eastern Limited, New Delhi (1987).

108874

Date Slip

This book is to be returned on the
date last stamped.

This image shows a blank sheet of white paper with horizontal ruling lines. A single vertical line runs down the center of the page, creating two equal-width columns. The horizontal lines are evenly spaced and extend across the entire width of the paper. There is no handwriting or other markings on the page.

ME-1990-M-VER-FIN.

Th

621.89

V59f